

Compton dragged gamma-ray bursts: the spectrum

Gabriele Ghisellini¹, Davide Lazzati,^{1,2} Annalisa Celotti³ and Martin J. Rees⁴

¹ *Osservatorio Astronomico di Brera, Via Bianchi 46, I-23807 Merate (Lc), Italy*

² *Dipartimento di Fisica, Università degli Studi di Milano, Via Celoria 16, I-20133 Milano, Italy*

³ *SISSA, Via Beirut 2-4, I-34014 Trieste, Italy*

⁴ *Institute of Astronomy, Madingley Road, Cambridge*

E-mail: gabriele@merate.mi.astro.it, lazzati@merate.mi.astro.it, celotti@sissa.it, mjr@ast.cam.ac.uk

11 November 2018

ABSTRACT

We calculate the spectrum resulting from the interaction of a fireball with ambient soft photons. These photons are assumed to be produced by the walls of a funnel in a massive star. By parameterizing the radial dependence of the funnel temperature we calculate the deceleration of the fireball self-consistently, taking into account the absorption of high energy γ -rays due to interaction with the softer ambient photons. The resulting spectrum is peaked at energies in agreement with observations, has a ν^2 slope in the X-ray band and a steep power-law high energy tail.

Key words: gamma rays: bursts — X-rays: general — radiation mechanisms: non-thermal

1 INTRODUCTION

We have recently proposed (Lazzati et al. 2000, hereafter Paper I) that the gamma-ray burst (GRB) phenomenon originates from the interaction of a relativistic fireball with a dense photon environment, leading to Compton drag. On one hand this is an inevitable effect if the progenitors of GRBs are massive stars which are about to explode or have just exploded as supernovae; on the other hand this mechanism greatly alleviates the efficiency problem faced by the standard internal shock scenario (Lazzati, Ghisellini & Celotti 1999; Panaitescu, Spada & Meszaros 1999; Kumar 1999). In Paper I we have discussed the basic Compton drag scenario, showing how this process can convert bulk motion energy directly into radiation with a remarkable high efficiency and, on the basis of simple estimates, how the resulting spectrum should peak, in a $\nu F(\nu)$ representation, around ~ 1 MeV, as observed.

Here we quantitatively and self-consistently estimate the predicted spectrum, assuming that the fireball propagates in a funnel inside a massive star, and show that, independently of the details of the model, it satisfactorily resembles what observed. Since the funnel walls emit a blackbody spectrum and the scattered photons are boosted by the square of the Lorentz factor (Γ) of the fireball, the local spectrum has a blackbody shape, at a temperature enhanced by Γ^2 . However, the observed spectrum, convolution of all the locally emitted spectra, is not a blackbody, due to four main effects: i) the funnel walls would not be at a uniform temperature, but there should be a gradient between the internal and external parts; ii) if the Compton drag process is efficient, the fireball decelerates; iii) the very high energy

emission produced in the internal regions can interact with the ambient photons, producing electron-positron pairs; iv) the fireball may become optically thin to scattering outside the funnel, where the ambient photons are characterized by the same temperature, but their energy density is progressively diluted with distance.

2 BASIC ASSUMPTIONS

We postulate that the fireball propagates with a bulk Lorentz factor Γ inside a funnel cavity, whose walls emit blackbody radiation at a temperature T , of conical shape with semi-aperture angle ψ . The calculation starts at the distance z_0 , assumed to be the end of the acceleration phase and, for consistency, we verify that the power emitted at $z < z_0$ is negligible.

We assume that the fireball is and remains cold in the comoving frame. At z_0 , in fact, the internal energy has been already used to accelerate the fireball, and thus protons are sub-relativistic. On the other hand leptons might be still hot at z_0 and/or being re-heated when the bulk scattering process starts to be efficient. However, in a few (Compton) cooling timescales they would reach the (sub-relativistic) Compton temperature. It is thus reasonable to treat also the leptonic component as cold in the estimate of both the dynamics and resulting spectrum.

The initial Lorentz factor (at z_0) is indicated as Γ_0 , and the fireball energy is therefore $E_f = \Gamma_0 M_f c^2$, where M_f is its rest mass. For simplicity, the dependence of the temperature on z , between z_0 and the radius of the star z_* , has been parameterized by a power law:

arXiv:astro-ph/0002049v2 20 Jun 2000

$$T(z) = T_0 \left(\frac{z}{z_0} \right)^{-b} = T_* \left(\frac{z}{z_*} \right)^{-b} \quad (1)$$

where T_* is the temperature at the top of the funnel.

Inside it, we approximate the local radiation energy density of the ambient photons as $U(z) = aT^4(z)$. Beyond z_* , and in the region where the fireball remains optically thick (i.e. for $z < z_T$, see below), $U(z)$ is characterized by the same temperature, but decreases. As the relevant quantity is the amount of radiation which is indeed scattered by the fireball, we parameterize the dependence on z of the product $U(z) \times$ (the scattering rate) as $(z/z_*)^{-g}$.

We consider g a free parameter. Inside the funnel $g = 0$, while outside it a value $g > 2$ can account for a decrease in the scattering rate due to the changing of the typical scattering angle (photons come preferentially at smaller angles as z increases). As the scattering rate is $\propto (1 - \beta \cos \theta)$, where θ is the angle between the photon and the electron directions, far from the star surface $(1 - \beta \cos \theta) \propto (z/z_*)^{-2}$, corresponding to $g \sim 4$. Furthermore some of the radiation produced by the massive star could be reflected and re-isotropized by scattering material, of unknown radial density profile, likely surrounding the massive star progenitor. In particular if this forms a wind with a z^{-2} profile, the energy density of the re-isotropized radiation scales as z^{-3} , and dominates the seed photon distribution at large distances. In this case $U(z) \times$ (the scattering rate) can have a complex profile, being flat in the vicinity of the surface of the star, then decreasing as z^{-2} and as z^{-4} for increasing z , to become flatter when the component associated with the re-isotropized photons dominates. It is also possible that, as a result of intermittent stellar activity, the stellar wind is not continuous. In this case a single shell may dominate the scattering, producing a homogeneous and isotropic scattered radiation field, dominating the total radiation energy density beyond some critical distance.

The distance z_T at which the fireball becomes optically thin to scattering is

$$z_T = \left(\frac{\sigma_T E_f}{\pi \psi^2 m_p c^2 \Gamma_0} \right)^{1/2} \sim 3.7 \times 10^{14} \psi_{-1}^{-1} E_{f,51}^{1/2} \Gamma_{0,2}^{-1/2} \text{cm} \quad (2)$$

where the conventional representation $Q = Q_x 10^x$ and c.g.s. units are adopted. It is then likely that the fireball becomes transparent at $z > z_*$ (since the radius of red supergiants is $z_* \lesssim 10^{13}$ cm).

As long as the fireball is opaque to scattering, the interaction with photons boosts their energy by a factor $\sim 2\Gamma^2$. Therefore the (local) total energy emitted by the fireball through the Compton drag process (over a distance dz) is

$$dE(z) = 2\pi \psi^2 z^2 a T_0^4 \left(\frac{z}{z_0} \right)^{-4b} \Gamma^2 dz \quad z < z_* \quad (3)$$

$$dE(z) = 2\pi \psi^2 z^2 a T_*^4 \left(\frac{z}{z_*} \right)^{-g} \Gamma^2 dz \quad z > z_*. \quad (4)$$

The factor 2 in front of the RHS of these equations takes into account that the preferred scattering angle is $\sim 90^\circ$, corresponding to an average energy boost of $2\Gamma^2$.

Let us now consider the spectral shape. For this it is convenient to use dimensionless photon energies and temperatures, defined as $x \equiv h\nu/(m_e c^2)$ and $\Theta \equiv kT/(m_e c^2)$, respectively.

The resulting Compton spectrum has a blackbody

shape, of effective temperature $T_c = 2\Gamma^2 T$ (or $\Theta_c = 2\Gamma^2 \Theta$), i.e. the local spectral distribution produced within dz is given by:

$$dE(z, x) = \pi^2 \psi^2 \frac{z^2}{\Gamma^6} m_e c^2 \left(\frac{m_e c}{h} \right)^3 \frac{x^3}{e^{x/\Theta_c} - 1} dz; \quad z < z_* \quad (5)$$

$$dE(z, x) = \pi^2 \psi^2 \frac{z^2 (z/z_*)^{-g}}{\Gamma^6} m_e c^2 \left(\frac{m_e c}{h} \right)^3 \frac{x^3}{e^{x/\Theta_{c,*}} - 1} dz; \quad z > z_*, \quad (6)$$

where $\Theta_{c,*} = 2\Gamma^2 \Theta_*$. Equations (5) and (6) are correctly normalized, i.e. the integrated energies correspond to those expressed in (3) and (4).

3 THE FIREBALL DYNAMICS

As long as the fireball remains optically thick for scattering and this occurs in the Thomson regime, the dynamics (deceleration) of the fireball due to the radiative drag, obeys:

$$M_f c^2 \frac{d\Gamma}{dz} = -2\pi \psi^2 z^2 a T^4 \Gamma^2. \quad (7)$$

Assuming the temperature profile of equation (1) we obtain:

$$\Gamma = \frac{\Gamma_0}{1 + 2\pi \psi^2 a T_0^4 \Gamma_0^2 z_0^3 [(z/z_0)^{3-4b} - 1]/[E_f(3-4b)]}; \quad z_0 < z < z_*, \quad (8)$$

and thus the deceleration radius, z_d , defined as the distance at which Γ is halved, corresponds to:

$$\begin{aligned} z_d &= z_0 \left[1 + \frac{E_f(3-4b)}{2\pi \psi^2 a T_0^4 \Gamma_0^2 z_0^3} \right]^{1/(3-4b)} \\ &= z_0 \left[1 + \frac{E_f(3-4b)}{2\pi \psi^2 a T_*^4 \Gamma_0^2 (z_*/z_0)^{4b} z_0^3} \right]^{1/(3-4b)} \end{aligned} \quad (9)$$

Beyond z_d , the Lorentz factor decreases with distance as a power law, whose slope is determined by the temperature profile.

Outside the star radius ($z > z_*$) the Lorentz factor follows:

$$\Gamma = \frac{\Gamma_*}{1 + 2\pi \psi^2 a T_*^4 \Gamma_* z_*^3 [(z/z_*)^{3-g} - 1]/[E_f(3-g)]}; \quad z_* < z < z_T. \quad (10)$$

Note that Klein-Nishina effects are important for incoming photon energies such that $x\Gamma > 1$, i.e. when $\Theta > 1/(3\Gamma)$. For simplicity, we neglect interactions in this regime when calculating $\Gamma(z)$, but we assume no scattering events when $\Theta > 1/(3\Gamma)$ in calculating the spectrum. This simplification is justified as long as most of the fireball energy is lost in the Thomson scattering regime (see Fig. 2, which shows that Γ starts to decrease at distances where the temperature is small enough to ensure scatterings entirely in the Thomson regime).

When the fireball becomes optically thin, the amount of scattered photons is correspondingly reduced, and the process becomes less efficient. As shown by equation (2), this is likely to happen at some distance from the star surface,

where the photon density is also reduced, thus further decreasing the efficiency of the process. In the numerical calculations we have however included the optically thin scattering regime, and one can see its contribution in Fig. 1 (dotted line).

4 PAIR PRODUCTION

A further effect which may strongly affect both the observed spectrum and the dynamics of the fireball is the production of electron–positron pairs through photon–photon interactions. Let us thus consider in turn the role of scattered and funnel radiation as seed photons for this process.

4.1 Interaction among photons in the beam

The threshold energy for interaction between photons of energies x and x_T is $x_T > 2/[x(1 - \cos\theta)] \sim 4\Gamma^2/x$, where all quantities are calculated in the observer frame. The latter expression takes into account that the high energy photons produced by the Compton drag are highly collimated, within a typical angle $\sin\theta \sim 1/\Gamma$. As the bulk of the scattered photons have energies $x \sim 2\Gamma^2(3\Theta)$, pair production would occur if $\Gamma\Theta > 1/3$.

However this also implies that the scattering process is in the Klein Nishina regime, and we can therefore conclude that photon–photon collisions among photons in the beam can only affect the high energy tail of the spectrum produced at each radius, while the emission at the peak is unaltered. We therefore neglect this effect.

4.2 Interaction between beam photons and funnel radiation

The interaction between the γ -rays produced by the Compton drag process and photons emitted by the funnel walls would occur at large angles, resulting in an average energy threshold $x_T > 1/x$. Since $x \leq \Gamma_0$, this absorption mechanism would be significant as long as the funnel walls produce a sufficient number of photons with energies $x_T > 1/\Gamma_0$.

Let us then estimate the photon–photon optical depth $\tau_{\gamma\gamma}$, by integrating the product of the photon–photon cross section $\sigma_{\gamma\gamma}(x, x_T)$ and the photon density above threshold $n_\gamma(x)$ over the γ -ray path, i.e. from the site of creation, z_1 , to infinity, and over the photon energies:

$$\tau_{\gamma\gamma}(z_1, x) = \int_{x_T}^{\infty} dx' \int_{z_1}^{\infty} \sigma_{\gamma\gamma}(x', x) n_\gamma(z, x') dz. \quad (11)$$

Since $\sigma_{\gamma\gamma}(x', x)$ is peaked at the threshold energy, equation (11) can be simplified (Svensson 1984, 1987) as

$$\tau_{\gamma\gamma}(z_1, x) = \frac{\sigma_T}{5m_e c^2} \int_{z_1}^{\infty} x_T U(z, x_T) dz, \quad (12)$$

where $U(z, x_T) = m_e c^2 n_\gamma(z, x_T)$ is the photon energy density at threshold, at the location z , i.e.

$$U(z_1, x_T) = \frac{8\pi h}{c^3} \left(\frac{m_e c^2}{h} \right)^4 \frac{x_T^3}{\exp[x_T/\Theta(z_1)] - 1}. \quad (13)$$

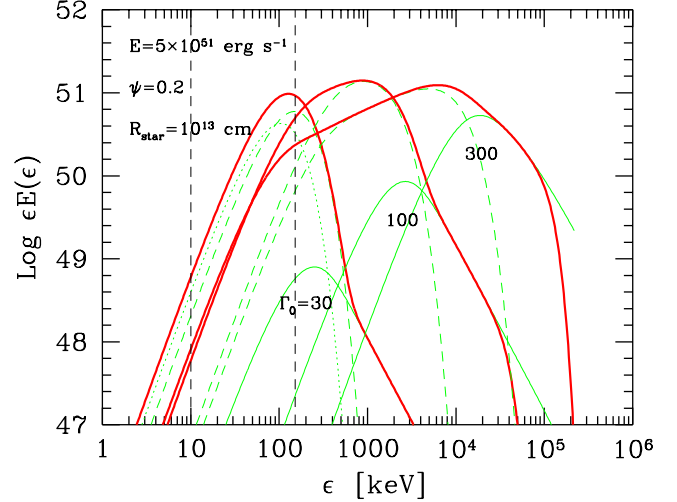


Figure 1. Example of spectra produced by Compton drag. The thick solid lines correspond to the sum of the radiation produced inside the funnel (thin solid lines) and outside it (dashed and dotted lines). The thin solid lines at the highest energies correspond to the emission neglecting photon–photon absorption, to show the importance of this process. The dotted line (only shown for the $\Gamma_0 = 30$ case) is the spectrum produced by the fireball once it becomes optically thin. The model parameters are for all cases: $E_f = 5 \times 10^{51}$ erg; $\psi = 0.2$; $b = 0.5$; $g = 2$; $z_* = 10^{13}$ cm and $T_* = 3 \times 10^5$ K. The three cases differ for the assumed initial bulk Lorentz factor and z_0 , i.e. $\Gamma_0 = 30, 100, 300$ and $z_0 = 3 \times 10^8, 10^9, 3 \times 10^9$ cm, respectively. The two vertical dashed lines mark 10 and 150 keV, the range of the foreseen hard X-ray detector onboard the Swift mission.

The radiation flux produced at the location z_1 is then decreased by the factor $\exp[-\tau_{\gamma\gamma}(z_1, x)]$ while crossing the funnel.

The absorbed radiation will be reprocessed by the pairs, and re-distributed in energy. Each electron and positron will have an energy $\gamma \sim x/2$ at birth, and will cool due to the Compton drag process. The positrons will then annihilate in collisions with the electrons in the fireball, producing a Doppler blueshifted annihilation line at $x \sim \Gamma$. We have neglected these reprocessing mechanisms, since, as can be seen in Fig. 1, the amount of energy absorbed in γ - γ collisions is small, amounting to a few per cent at most.

5 THE SPECTRUM

The observed total spectrum can be computed by integrating equations (3) and (4) over z , taking into account photon–photon absorption. The contribution produced within the star is given by:

$$E(x) = \pi^2 \psi^2 m_e c^2 \left(\frac{m_e c}{h} \right)^3 \int_{z_0}^{z_*} \frac{z^2 x^3 e^{-\tau_{\gamma\gamma}(z, x)}}{\Gamma^6 (e^{x/\Theta_c} - 1)} dz; \quad z_0 < z < z_*, \quad (14)$$

while beyond z_* the number of target photons able to interact with high energy γ -rays to produce pairs is negligible,

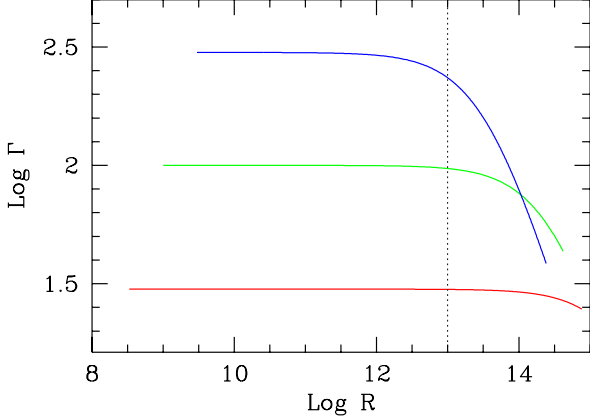


Figure 2. The profile of the bulk Lorentz factor Γ corresponding to the cases shown in Fig. 1. The vertical dotted line marks 10^{13} cm, the top of the funnel.

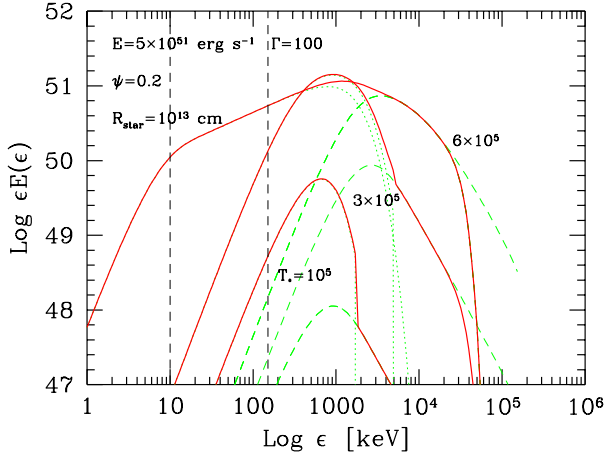


Figure 3. Spectra produced by Compton drag for three different choices of the temperature of the surface of the massive star (as labeled). For all cases $E_f = 5 \times 10^{51}$ erg; $\psi = 0.2$; $b = 0.5$; $g = 2$; $z_* = 10^{13}$ cm, $\Gamma_0 = 100$ and $z_0 = 10^9$ cm.

and thus, ignoring photon–photon absorption, we obtain:

$$E(x) = \pi^2 \psi^2 m_e c^2 \left(\frac{m_e c}{h} \right)^3 \int_{z_*}^{z_T} \frac{z^2 (z/z_*)^{-g} x^3}{\Gamma^6 (e^{x/\Theta_{c,*}} - 1)} dz; \quad z_* < z < z_T. \quad (15)$$

In Fig. 1 we show three examples of the predicted spectrum corresponding to different values of the initial bulk Lorentz factors. To illustrate the main features of the model and the importance of photon–photon absorption, this is calculated both with and without the photon–photon absorption term. Together with the total spectrum, the separate contributions for $z < z_*$ and for $z_T < z < z_*$ are reported. In Fig. 2 we show the corresponding Γ profiles. The effect of the star surface temperature (and of the entire funnel, since the parameter b is assumed to be the same for all cases) can be clearly seen in Fig. 3. Note the $\nu^{-1/2}$ power law shape in the X–ray band for the high temperature case. The extension of this power law branch depends on the value of g . In

the case shown ($g = 2$) the radiation energy density outside the funnel remains sufficiently large to cause the deceleration of the fireball, and this is responsible for the power law tail between 10 and 100 keV. For larger g the extension of this power law would decrease. This effect can also be seen for the high Γ_0 case in Fig. 1.

In order to determine the general features of the predicted spectrum and thus assess its robustness against the parameters of the model, we also derived analytical (although approximated) expressions for the spectral energy distribution.

5.1 Analytical approximations

First, let us approximate the blackbody spectral form with its Rayleigh–Jeans part, and let us neglect photon–photon absorption. In this case, for $x < 6\Theta^2$ we have:

$$\begin{aligned} dE(z, x) &\propto \frac{T}{\Gamma^4} z^2 dz; & \text{for } z_0 < z < z_* \\ &\propto \frac{T}{\Gamma^4} z^{2-g} dz; & \text{for } z_* < z < z_T. \end{aligned} \quad (16)$$

Three regimes occur at different distances:

$z_0 < z < z_d$: — in this case $\Gamma = \text{const}$, and integration over z yields:

$$E(x) \propto x^{-(3-3b)/b}; \quad \text{for } z > z_d \quad (17)$$

which, for $b = 0.5$, gives $E(x) \propto x^{-3}$.

$z_d < z < z_*$: — here Γ decreases as $(z/z_0)^{-(3-4b)}$ and thus:

$$E(x) \propto x^{-3(1-b)/(6-7b)} \quad \text{for } z_d < z < z_*; \quad (18)$$

which, for $b = 0.5$, results in $E(x) \propto x^{-3/5}$.

$z_* < z < z_T$: — at these distances the ambient radiation energy density decreases as $(z/z_0)^{-g}$. If Γ remains constant ($= \Gamma_*$), the spectrum $E(x) \propto x^2$, while, for Γ decreasing as $\Gamma \propto (z/z_0)^{-(3-g)}$

$$E(x) \propto x^{-1/2} \quad \text{for } z_* < z < z_T, \quad (19)$$

which is independent of g .

In conclusion, in the case of efficient Compton drag, and independently of the particular choice of parameters, the predicted spectrum is always characterized (in order of decreasing energy) by: a steep high energy tail; a first break flagging the deceleration of the fireball; a second break corresponding to radiation produced at the top of the funnel – above which the temperature of the ambient photons remains constant; a third break, below which the spectrum $\propto x^{-1/2}$, corresponding to the deceleration of the fireball due to the isothermal photon bath; and finally a fourth break, below which the spectrum $F(x) \propto x^2$. One obtains such a hard spectrum, instead of the familiar slope $F(x) \propto x$ corresponding to scatterings of isotropically distributed electrons and seed photons, because only the photons scattered along the forward direction are observed^{*}.

^{*} This can be seen by integrating Eq. 7.23 of Rybicki & Lightman (1979), in the angle range $[0 < \theta_1 < 1/\Gamma]$

6 DISCUSSION

If the fireball propagates in a dense photon environment the Compton drag effect must necessarily be taken into account, and it may even be the dominant emission mechanism, able to decelerate the fireball without the need of internal shocks and without invoking the build-up of large magnetic fields.

In this letter we have shown that the predicted spectrum, rather than being simply a black body spectrum boosted in energy, has a complex shape, with power law segments corresponding to the decrease in temperature of the funnel, deceleration of the fireball, and dilution of the radiation energy density as the fireball propagates outside the funnel while remaining optically thick.

The general features of the predicted spectrum qualitatively agree with observations, since they can explain the steep power law high energy tail, the peak of the emission, and a hard tail in the X-ray band. The latter feature is particularly interesting, since other models made different predictions. In the standard internal shock synchrotron model, in fact, the spectrum cannot be harder than $\nu^{1/3}$ in the thin part, and it is very unlikely that self-absorption can take place in the X-ray band (Granot, Piran & Sari 2000). This would in fact imply a huge density of relativistic particles, making the inverse Compton effect largely dominate the total radiation output. This radiation would be emitted at higher and yet unobserved frequencies, and would then worsen the already severe efficiency problem.

In the quasi-thermal Comptonization model, on the other hand, the typical predicted spectral shape in the X-ray band is $\propto \nu^0$, down to the typical frequencies of the seed soft photons, i.e. the IR-optical band (Ghisellini & Celotti 1999; Meszaros & Rees 2000).

The existing observations of a significant fraction of burst spectra harder than $\nu^{1/3}$ (Preece et al., 1999a,b; Crider et al., 1997) are therefore already a challenge to existing models, and may suggest a Compton drag origin of this portion of the spectrum. However the situation is not already a clear-cut because, to receive enough photons to study the spectral shape, integration times are much longer than the dynamical time-scales of the system, with the spectrum rapidly evolving in time. More sensitive instruments, such as the Burst Alert Telescope (BAT, a coded mask detector more sensitive than BATSE) onboard the foreseen Swift satellite will probably overcome this limitation.

We must also stress that the Compton drag scenario is not alternative to the more conventional internal shock one. Indeed, the front of the fireball will decelerate first, plausibly causing subsequent un-decelerated parts to shock even if the central engine is working in a continuous way. This would produce additional radiation, either by the synchrotron and inverse Compton processes or by quasi-thermal Comptonization, depending on the details of the particle acceleration mechanism (see Ghisellini & Celotti 1999). We then expect spectral evolution: since the latter radiation mechanisms produce a steeper low energy tail, a hard-to-soft transition (i.e. from ν^2 to $\nu^{1/3}$ or ν^0) would occur.

In this paper, we have considered the illustrative case of a single fireball moving out through an extended stellar envelope, along a funnel which is empty of matter but pervaded by thermal radiation from the funnel walls. The fireball itself (for typical parameters) remains optically thick until it

expands beyond the stellar surface. A burst with complex time-structure could be modeled by a series of fireballs or expanding shells. However, in this more general case, the later shells would suffer less drag, since not enough time may have elapsed to replenish the entire funnel cavity with seed photons. Indeed one expects the spikes to be more powerful the longer is the time interval between them, as more seed photons could pervade the cavity. This, besides causing internal shocks with the first shell which has been efficiently decelerated by Compton drag, will also result in a distribution of Γ -factors: they will become greater on axis, where few seed photons can efficiently Compton drag the shells, and smaller towards the border of the funnel, where seed photons can be replenished by the funnel walls.

We plan to investigate these possibilities and their consequences on the associated predicted afterglows in future work.

ACKNOWLEDGMENTS

AC acknowledges the Italian MURST for financial support.

REFERENCES

- Crider A. et al., 1997, ApJ, 479, L39
- Ghisellini G., Celotti A., 1999, ApJ, 511, L93
- Granot J., Piran T., Sari R., 2000, ApJ, 534, L163
- Kumar P., 1999, ApJ, 523, L113
- Lazzati D., Ghisellini G., Celotti A. & Rees M.J., 2000, ApJ, 529, L17 (Paper I)
- Lazzati D., Ghisellini G. & Celotti A., 1999, MNRAS, 309, L13
- Meszaros P. & Rees M.J., 2000, ApJ in press, astro-ph/9908126
- Panaitescu A., Spada M. & Meszaros P., 1999, ApJ, 522, L105
- Preece R.D. et al., 1998a, ApJ, 496, 849
- Preece R.D. et al., 1998b, ApJ, 506, L23
- Rybicki G.B. & Lightman A.P., 1979, Radiative Processes in Astrophysics, J. Wiley & Sons (New York)
- Svensson R., 1984, MNRAS, 209, 175
- Svensson R., 1987, MNRAS, 227, 403